

**Emergence of collective changes in travel direction of starling flocks
from individual birds fluctuations**

Alessandro Attanasi^{1,2}, Andrea Cavagna^{1,2,3}, Lorenzo Del Castello^{1,2}, Irene Giardina^{1,2,3}‡, Asja Jelic^{1,2}‡,*
Stefania Melillo^{1,2}, Leonardo Parisi^{1,2,4}, Oliver Pohl^{1,2},† Edward Shen^{1,2}, and Massimiliano Viale^{1,2}

¹ *Istituto Sistemi Complessi, Consiglio Nazionale delle Ricerche, UOS Sapienza, 00185 Rome, Italy*

² *Dipartimento di Fisica, Università Sapienza, 00185 Rome, Italy*

³ *Initiative for the Theoretical Sciences, The Graduate Center,
City University of New York, 10016 New York, USA*

⁴ *Dipartimento di Informatica, Università Sapienza, 00198 Rome, Italy and*

‡ *e-mail: asja.jelic@gmail.com, irene.giardina@roma1.infn.it*

COLLECTIVE TURNS

Acceleration curves and ranking. As discussed, in the Methods part of the paper, by sampling at 170Hz, without filtering, the wing flapping motion (with the frequency $\omega_{\text{flap}} = 10\text{Hz}$) would completely dominate acceleration, while instead we are interested in capturing a signal of changes in the travel direction. By applying a second-order low-pass digital Butterworth filter on the velocities, typically with a cutoff frequency $\omega_{\text{flap}}/30$, obtained accelerations capture the low frequency corresponding to the turn which can then be detected by a strong peak in the acceleration curves $\mathbf{a}_i(t)$. The acceleration curves obtained in this way are shown in Fig.S1 for some of the turning events. Comparison of the acceleration curves gives us time delays in turning between each pair of birds in a flock, from which we can calculate the order and time of turning of each bird. We can therefore say who is the first to turn, who is second, and so on. More details of the ranking procedure are given in ref. [1].

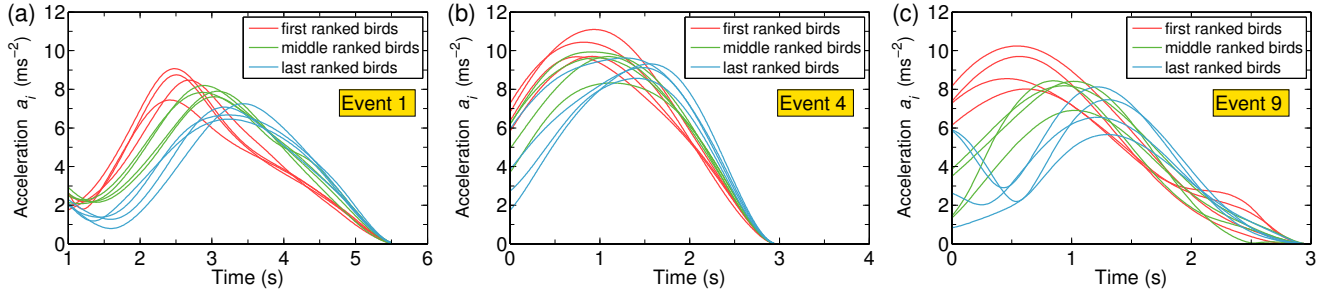


FIG. S1. **Acceleration curves.** For three turning events labelled E1, E4, and E9 (for details see Supplementary Table S1), we plot accelerations of several birds during the turning event. Birds are colored according to their turning time delay, i.e. whether they are among the first ranked birds (red), middle ranked birds (green), or the last ranked birds (blue). Note that for most of the turning events the acquisition of data started not long before the turn itself started, while only for a few events (e.g. event E1 in panel (a)) we were able to capture and track long enough time before the turn.

* Present address: The Abdus Salam International Centre for Theoretical Physics (ICTP), Strada Costiera 11, 34014 Trieste, Italy.

† Present address: Institut für Theoretische Physik, Technische Universität Berlin, Hardenbergstrasse 36, D-10623 Berlin-Charlottenburg, Germany.

REORIENTATION DURING TURNS

Global orientation of the flock

Turning plane. It has previously been observed that the trajectories of birds during a turn lie approximately on a plane (see ref. [1] and Fig.1-a). We exploit this fact in order to simplify the representation of a turn propagation through the flock and subsequent analysis. We determine the ‘turning plane’ by using two average flock velocity vectors: $\mathbf{V}_1 \equiv \mathbf{V}(t_1)$ at time $t = t_1$ of the start of the turn, and $\mathbf{V}_2 \equiv \mathbf{V}(t_2)$ at time $t = t_2$ shortly after the turn is finished. The average flock velocity at time t is calculated as $\mathbf{V}(t) = \frac{1}{N} \sum_{i=1}^N \mathbf{v}_i(t)$, where $\mathbf{v}_i(t)$ is the velocity of bird i at time t . The ‘turning plane’ can then be defined by its normal unit vector \mathbf{n}_3 which is perpendicular to the plane, and the flock’s barycenter position at time t_1 . Vector \mathbf{n}_3 is obtained as a unit vector orthogonal to \mathbf{V}_1 , as well as to \mathbf{V}_2 , that both lie within the ‘turning plane’, that is $\mathbf{n}_3 = (\mathbf{V}_1 \times \mathbf{V}_2) / \|\mathbf{V}_1 \times \mathbf{V}_2\|$. Finally, the normal to the plane \mathbf{n}_3 , together with a unit vector $\mathbf{n}_1 = \mathbf{V}_1 / \|\mathbf{V}_1\|$ along the direction of motion at the start of the turn t_1 , and a unit vector $\mathbf{n}_2 = \mathbf{n}_3 \times \mathbf{n}_1$, form an orthogonal coordinate system $(\mathbf{n}_1, \mathbf{n}_2, \mathbf{n}_3)$ (see Fig.1-a). We typically use this coordinate system $(\mathbf{n}_1, \mathbf{n}_2, \mathbf{n}_3)$ for data visualization in the paper. Note that times t_1 and t_2 are not necessarily initial and final times of the acquisition, but the times before and after the flock turns. They are estimated either from the trajectories themselves, or from the calculated velocities and radial accelerations.

During the turn, between t_1 and t_2 , the flock turns on the above defined turning plane. This can be verified by looking at the scalar product between the unit vector of velocity (representing direction of motion) and the normal to the plane \mathbf{n}_3 . Indeed, in Fig.S2 one can see that this scalar product, $\mathbf{n}_3 \cdot \mathbf{V}(t)/V(t)$, fluctuates around zero, thus confirming the ‘turning plane’ observation. Other scalar products of interest are also given, such as: $\mathbf{V}(t) \cdot \mathbf{n}_1$ that quantifies the change of the flock’s direction of motion over time with respect to the start of the turn at $t = t_1$, and $\mathbf{V}(t) \cdot \mathbf{G}$ (with \mathbf{G} being gravity unit vector) that shows whether a flock is flying parallel to the ground or not.

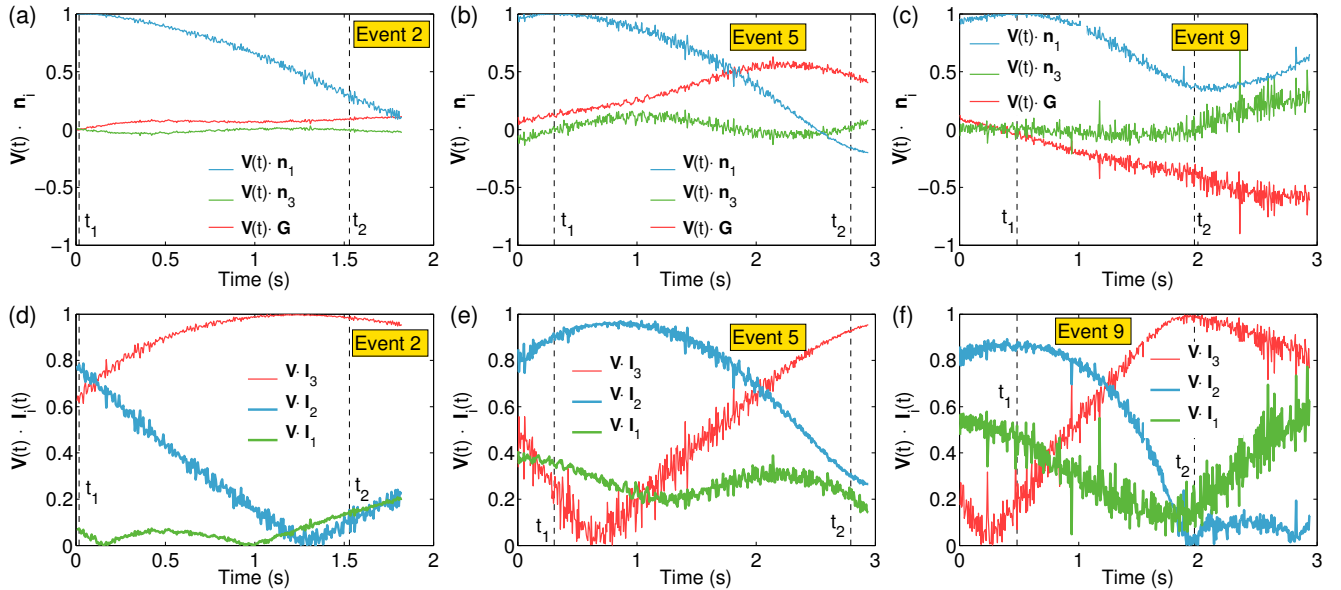


FIG. S2. **Flock’s direction of motion and orientation during turning events.** For three turning events labelled E2, E5, and E9 (for details see Supplementary Table S1), we study the change in the flock’s direction of motion and its orientation in space during a turn. Times: $t = t_1$ of the start of the turn, and $t = t_2$ after the turn are marked by vertical dashed lines. Panels (a), (b), (c) on the top show how the flock’s global direction of motion, given by a unit vector of its velocity $\mathbf{V}(t)$, changes over time with respect to three characteristic directions: i) direction of motion at the start of the turn t_1 given by a unit vector \mathbf{n}_1 , ii) normal to the ‘turning plane’ \mathbf{n}_3 , and iii) gravity given by a unit vector \mathbf{G} . Scalar product $\mathbf{V}(t) \cdot \mathbf{n}_1$ (blue curve) quantifies how much the direction of motion changes during the turn: it is 1 at time t_1 , while its final value corresponds to the angle between the initial and final direction of motion. The value of the scalar product $\mathbf{V}(t) \cdot \mathbf{n}_3$ (green curve) fluctuates around 0 during the turn between times t_1 and t_2 , confirming that the turn lies on a ‘turning plane’ given by its normal vector \mathbf{n}_3 . Finally, scalar product $\mathbf{V}(t) \cdot \mathbf{G}$ (red curve) shows whether the flock is turning parallel to the ground (values around 0) or not. Panels (d), (e), (f) on the bottom show the evolution of the relation between the flock’s global direction of motion (given by its velocity unit vector $\mathbf{V}(t)$) and its elongation axes \mathbf{I}_1 , \mathbf{I}_2 , and \mathbf{I}_3 over the time of the turn.

Elongation axes. It is convenient to consider the three principal elongation axes of the flock \mathbf{I}_1 , \mathbf{I}_2 , and \mathbf{I}_3 . Since flocks typically have asymmetric flat shapes the dimensions of the group along these axes are $I_1 < I_2 < I_3$. The smallest dimension I_1 characterizes the thinness of the flock and its relative axis \mathbf{I}_1 defines the yaw axis of the flock. Flocks typically fly parallel to the ground with their yaw axis parallel to gravity (see [2] and Supplementary Table S1). To study the re-orientation of the flock during the turn, we computed the angles between the three axes and the flock’s velocity and checked their evolution in time from the start to the end of the turn (see Fig.S2). Since turns are almost planar, a concise description of this dynamics is given by the normalized scalar product of the longest elongation axis \mathbf{I}_3 and the flock’s velocity before and after the turn, i.e. at times t_1 and t_2 for all our turning events. The result is displayed in Fig.6, and confirms what is qualitatively observed in Fig.2. The values of these scalar products reported in Supplementary Table S1 confirm that prior to the turn flock’s longest axis tends to be almost perpendicular to the direction of motion (small values $\mathbf{I}_3 \cdot \mathbf{V}_1$, so that angle between them is $\gtrsim 60^\circ$), while after the turn, the longest axis and the flock’s velocity become much more aligned as the angle between them reduces (large values $\mathbf{I}_3 \cdot \mathbf{V}_2$).

Typically, the values of the scalar product $\mathbf{I}_3 \cdot \mathbf{V}$ at the start of the turn t_1 are below 0.5, corresponding to an angle between 60° and 90° between the longest axis and velocity. There are a few exceptions to this general conclusion, which can be easily explained. On the one hand, the exceptions are events E11 and E12 which correspond to two consecutive turns of the same flock, and occur after a merging of two separate flocks into one (as revealed by the original videos of the events), which might be the reason why the reorientation is different. In addition, for these two events we find that the longest elongation axis \mathbf{I}_3 is more aligned to gravity \mathbf{G} than the yaw axis \mathbf{I}_1 , contrary to all other flocks we analyzed (see Supplementary Table S1) and results in [2]. On the other hand, for event E2, the data acquisition initiated too late to capture the very start of the turn. Although this did not hinder the determination of the ranking curve, the orientation of the flock already started to change prior to the start of the acquisition, preventing us from obtaining the initial orientation angle.

Origin of the turn. In Supplementary Table S1, we give values for other quantities that give additional information about the position of the origin of the turn. For example, we can look at the normalized scalar product between \mathbf{d}_0 and the flock’s velocity \mathbf{V}_1 at the start of the turn (see column $\mathbf{V}_1 \cdot \mathbf{d}_0/d_0$ in Supplementary Table S1). Its low values indicate that in most events the initiating birds are situated on the sides of the flock and not in the front or in the back, consistent with our previous analysis of Fig.3. In the same way, we can calculate the normalized scalar product between \mathbf{d}_0 and the velocity \mathbf{V}_2 assumed by the flock *after* the turn (column $\mathbf{V}_2 \cdot \mathbf{d}_0/d_0$ in Supplementary Table S1). For most of the flocks, this product is negative suggesting that once the top ranked birds initiate the turn they try to move towards the center of the flock, therefore “pushing” the whole flock to turn in the direction opposite to vector \mathbf{d}_0 as visually displayed in the flocks’ projections of Fig.2 and Fig.S2.

Propagation during turns

In Fig. S3 we show how the information to change the direction of motion propagates from the first bird through an entire flock. In the same way as in Fig.2, we project the birds' positions at the start of the turn to the 'turning plane' coordinate system $(\mathbf{n}_1, \mathbf{n}_2, \mathbf{n}_3)$ centered at the flock's barycenter at time t_1 . The color used for each bird reveals its turning time delay t_i with respect to the first bird to turn to which we assign the delay $t_1 = 0$ s. The values of the time delays are used from the established ranking in ref. [1].

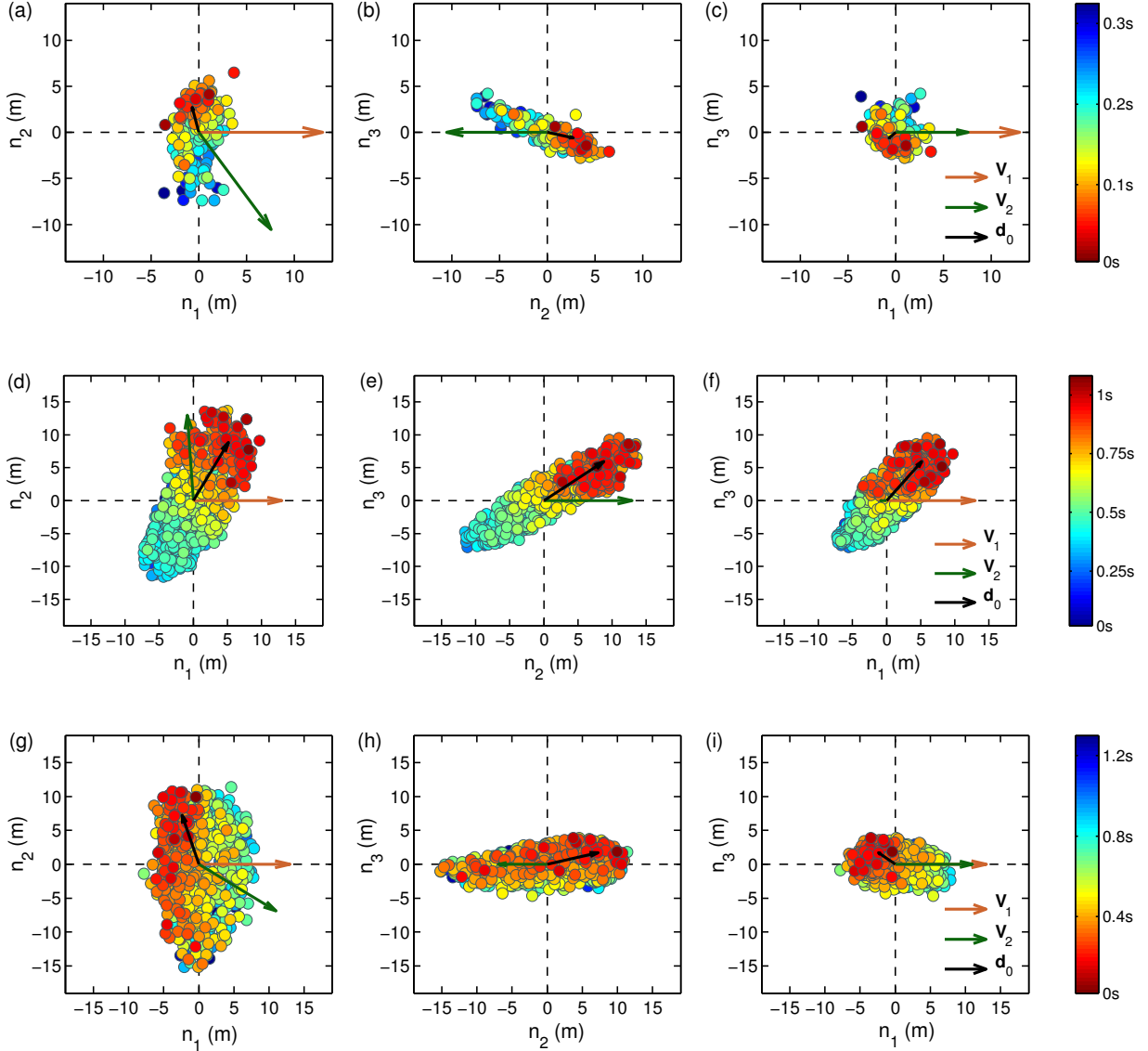


FIG. S3. **Propagation of the turn through a flock.** We show propagation of the turn through a flock for several different turning events: event number E4 in top panels; event number E6 in middle panels; event number E10 in bottom panels. The flocks are shown at moment t_1 of the start of their turn by using the projections on the planes of the 'turning plane' orthogonal system $(\mathbf{n}_1, \mathbf{n}_2, \mathbf{n}_3)$ centered at the flock's center of mass. Different panels show a view on the flocks (a), (d), (g) from the top, (b), (e), (h) from the front, and (c), (f), (i) from a side. At time t_1 each flock is moving along the direction n_1 with velocity \mathbf{V}_1 , which is to the right in panels (a), (d), (g) and (c), (f), (i), while in panels (b), (e), (h) they move towards the viewer. At moment t_2 after the turn, each flock is moving with the velocity \mathbf{V}_2 . The velocity vectors are rescaled (increased), in order to emphasize the old and new direction of global flock's movement. A wave of directional change information spreads through each of the flock during a turn. The birds are colored according to their turning time delays t_i , as indicated by the colorbar on the right. The mean position of the first 5 birds to turn at time t_1 , with respect to the barycenter, is indicated by vector \mathbf{d}_0 .

Equal radius paths and network rearrangement

Trajectories of individual birds of a flock performing a collective turn show that birds follow paths of very similar radii of curvature, causing their trajectories to cross (see Fig.5). Having detailed 3D trajectories allows us to be more quantitative in our characterization of this phenomena. Let us call $\mathbf{r}_{ij} = \mathbf{r}_j - \mathbf{r}_i$ the position of bird j relative to bird i . We can monitor the orientational change of \mathbf{r}_{ij} between the initial time $t = 0$ of the event and a later time t . This is described by the angle θ_{ij} between the two vectors $\mathbf{r}_{ij}(0)$ and $\mathbf{r}_{ij}(t)$

$$\cos \theta_{ij}(t) = \frac{\mathbf{r}_{ij}(0) \cdot \mathbf{r}_{ij}(t)}{\|\mathbf{r}_{ij}(0)\| \|\mathbf{r}_{ij}(t)\|}. \quad (\text{S1})$$

Averaging over all pairs of birds i and j , we obtain $\theta_r = \langle \theta_{ij} \rangle_{i,j}$, which quantifies the angular variation of the whole structural network of birds over time. In Fig. S4-a we show the evolution over time of $\theta_r(t)$ and we compare it with $\theta_V(t)$, the angle between the global direction of motion of the flock at time t and the one at time $t = 0$. The interesting point is that for parallel path turning the angles θ_r and θ_V must be highly correlated, with $\theta_r = \theta_V$ in the rigid-body limit. On the contrary, we find that while the angle θ_V increases strongly during the turn, measuring a change of the flock's direction of motion, angle θ_r does not change considerably. Other turning events show similar behaviour, with small changes in θ_r over the time scales of the analyzed turns, see Fig.S4-b. Small changes in the angular variation of the network of the flock mean that the birds adapt the new direction of motion with no changes in their relative positions with respect to the absolute reference frame, a characteristic of the equal radius path turning. We show this illustratively in Fig.6-a,b. As discussed in the main text of the paper, reorientation of the birds in the flock in this way not only enables efficient and fast turning of a flock as a collective, it also significantly changes the positional role of individuals within the flock, so as to alternate risky positions over time.

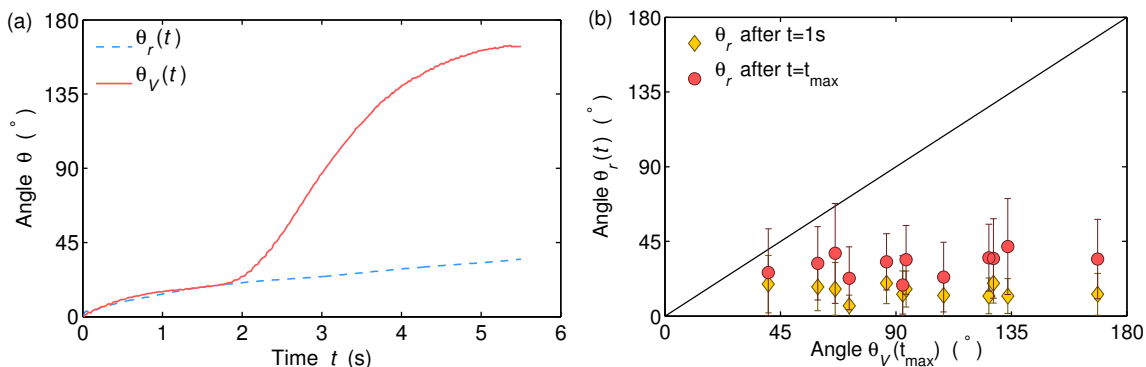


FIG. S4. **Equal radius turning.** (a) Temporal evolution of the angles $\theta_r(t)$, which measures the angular variation of the structural network of birds (dashed blue line), and $\theta_V(t)$, the angle between the flock's velocity $\mathbf{V}(t)$ and $\mathbf{V}(t = 0)$ (solid red line), for turning event E1 (flock 20110208_ACQ3). (b) For all 12 events, on the x-axis we plot the maximal change of the flock's travel direction $\theta_V(t_{\max})$ calculated at final time $t=t_{\max}$ of the acquisition, while on the y-axis we plot two values of the angular variation of the network θ_r calculated at: (i) $t = 1$ s after the start of the acquisition (yellow diamonds), and (ii) at the final time of the turning event $t = t_{\max}$ (red circles). All turning events show similar behavior with the angular variation θ_r being small compared to the maximal change of the direction of motion θ_V .

INDIVIDUAL DEVIATIONS FROM THE GLOBAL DIRECTION

Dealignment time factor. We define the dealignment time factor $\delta_i(\tau)$ as a percentage of time during a time interval of length τ before the start of the turn t_1 , during which bird i deviates from the mean direction of motion more than a given threshold value C_0

$$\delta_i(\tau) = \frac{1}{\tau} \sum_{t=t_1-\tau}^{t_1} \Theta(C_0 - C_i(t)). \quad (\text{S2})$$

Here, $\Theta(x)$ is a Heaviside step function, so that $\Theta(x) = 0$ for $x < 0$, and $\Theta(x) = 1$ for $x > 0$. For the threshold value C_0 , we choose a median of the set of values $\{C_i(t) | i = 1, \dots, N; t \in [t_1 - \tau, t_1]\}$. In that case, the dealignment time factor $\delta_i(\tau)$ gives the percentage of time during the time interval τ for which bird i was more dealigned with the global direction of motion than at least 50% of other birds in the flock. Note that other thresholds can be also considered. We checked several other threshold values, below and above the median value. However, no qualitative difference was observed, as long as the threshold was meaningful. For example, value of C_0 that is too close to the minimum of all $C_i(t)$, can not produce good statistics, as it describes extreme deviations from the average behaviour which are very rare. Values of C_0 that are too high, i.e. too close to 1, are also not suitable, as most of the birds are not perfectly aligned to the global direction and one would not distinguish between meaningful deviations and deviations due to wing flapping. Note that the average of all the values of the threshold C_0 for different events, when chosen as a median of all $C_i(t)$ within the above defined period of time τ prior to the turn, is already very high, 0.992, which is in accordance with a very strong polarization of the flocks. However, even when the choice of C_0 is closer to the extreme values, the birds that are deviating more persistently from the average behaviour are still the ones having large $\delta_i(\tau)$. For some turning events, choosing a threshold value that is somewhat larger or smaller than the median value, but not for too much, produced clearer distinction between these persistently deviating birds and others. Nevertheless, for the sake of uniformity and generalization, we present the results using a median as a threshold value C_0 for all of the analyzed turning events.

As discussed in Section II C, we find a strong correlation between the location of an individual within the flock and the value of its dealignment factor: the farther away a bird is along the lateral elongation axis \mathbf{I}_3 , the more frequently it exhibits consistent fluctuations from the global direction of motion. We do not find, however, any obvious correlation when looking at the birds' positions along the other two elongation axes, as shown in Fig. S5-a,b where we plot $\delta_i(\tau)$ as a function of the bird's position along other two axes \mathbf{I}_2 and \mathbf{I}_1 . There is also no correlation between $\delta_i(\tau)$ and the birds' position along the direction of motion \mathbf{n}_1 , that is, whether it is situated in the front or in the back of the flock (see Fig. S5-c). The only correlation can be found between $\delta_i(\tau)$ and the lateral (left-right) direction \mathbf{n}_2 direction, which is not surprising as we showed that the longest elongation axis \mathbf{I}_3 is almost parallel to it at the start of the turn t_1 , (see Fig. S5-d).

Dealignment amplitude. We also define a normalized dealignment amplitude $\Delta C_i/C_0$, where ΔC_i is a maximal deviation from the mean flock's direction of motion performed by bird i during the time interval τ before the start of the turn

$$\Delta C_i = C_0 - \min\{C_i(t) | C_i(t) < C_0; t \in [t_1 - \tau, t_1]\}. \quad (\text{S3})$$

We note that the velocities of individual birds $\mathbf{v}_i(t)$ are calculated from the individual trajectories of each bird i , by looking at its positions at the frequency of 10hz and not at the sampling frequency 170hz (however, we used all the available data points sampled at 170hz). This is because, as stated above, at such a high frequency of 170hz the deviations from the mean direction of motion would include the zig-zag part of the trajectories which are due to wing-flapping. We avoid this by choosing to calculate the velocities at the time interval of 0.1s, i.e. at 10hz which is exactly the frequency of the flapping. Finally, we present the data for the time interval $\tau = 1$ s before the start of the turn at moment t_1 . However, for the turning events in which the turn starts at moment $t_1 < 1$ s from the start of the acquisition, the time interval τ starts from the beginning of the acquisition and, therefore, includes also time t_1 . Typically, we use time period of $\tau = 1$ s which is short enough so that the results are not strongly influenced by this lack of data before the start of the turn, but long enough to give good statistics for dealignment.

In Section II C, we show that the top-ranked individuals, which are situated close to one edge of the flock, are among the individuals with the highest realignment factor $\delta_i(\tau)$. On the contrary, we find that there is not such a correlation between the dealignment amplitude $\Delta C_i/C_0$ and the location of an individual within the flock. Here we show this for some of the other turning flocks, see Fig. S6, confirming our conclusion that what triggers the turn is the presence of a repeated deviation from the flock's global direction and not the strength of a single, momentary deviation from the average behaviour.

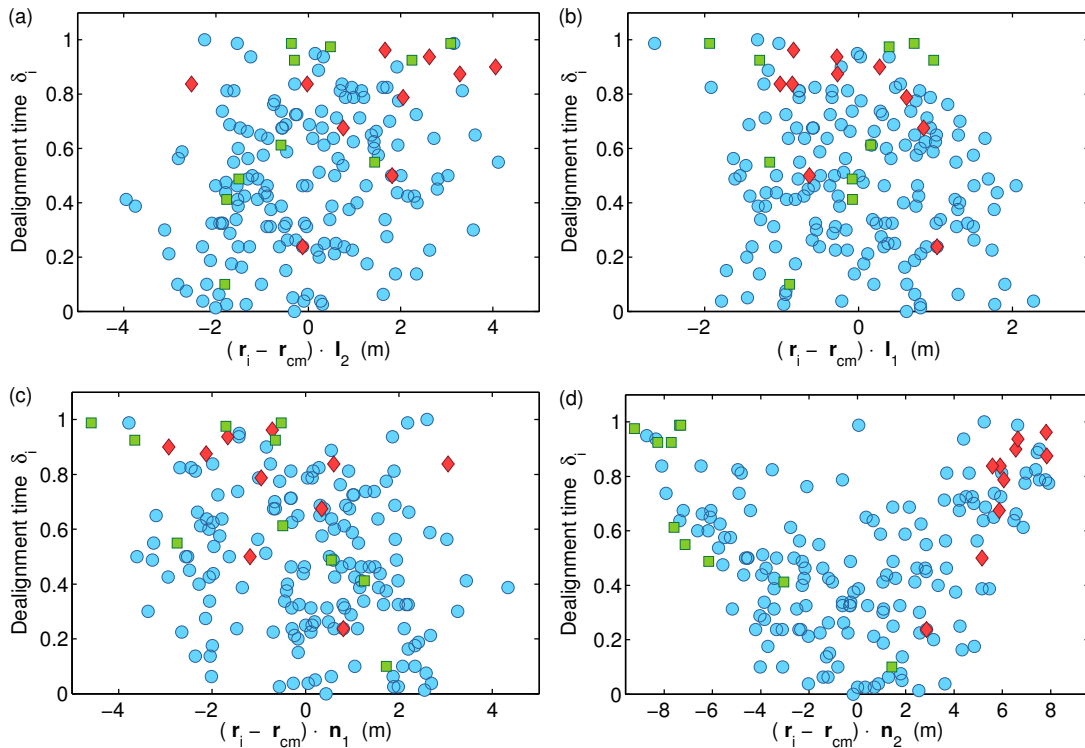


FIG. S5. **Dependence of the bird's deviations from the global direction of motion on its location within the flock.** For event E1, dealignment time factor $\delta_i(\tau)$ is plotted as a function of position of bird i along the elongation axes (a) \mathbf{I}_2 and (b) \mathbf{I}_1 , with respect to the flock's center of mass at the moment the turn is initiated t_1 . No strong dependence between the dealignment time factor $\delta_i(\tau)$ and position along these two elongation axes is found. We also check the dependence on the position along (c) the direction of motion (front-back), and (d) transverse direction (left-right), the latter being almost the same as the longest elongation axis \mathbf{I}_3 . The top ten ranked birds (red diamonds) and the last ten birds to turn (green squares) are marked.

Outward and inward deviations. In this paper we show that, while flying straight, flocks typically acquire asymmetric shapes, with their longest elongation axis being oriented perpendicular to the flock's velocity. Moreover, the results in Section II C demonstrate that birds deviate more and more frequently from the common flock direction, when being positioned closer and closer to the lateral edges of the flock. Here we contribute to these conclusions by distinguishing between the direction of these deviations, that is, whether they are directed towards the void space outside of the flock, or towards the inside of the flock where the space is occupied with other birds. For many flocks we find that most of the deviations performed by the birds closer to the elongated edges are towards the boundary of the flock (outward), and not towards the center of the flock (inward), as for the turning event E1 shown in Fig.S7-a,b. This result is consistent with the maximal diffusion along the wing's axis found in [3], and, in particular, the dynamics of the border. As discussed therein, the dynamics of the edge birds results from balancing the availability of void space outside the flock, staying at the border of a flock rather than going astray [4], and the reluctance of their internal neighbours to give up a more favourable position. Finally, as this effect builds up in time, some of these birds successfully manages to move inwards, compensating the feedback to average motion,. This incites a response of their neighbours, followed by a collective turn of the whole flock. In fact, in some of the turning events, we could clearly detect the inwards fluctuations performed by the top-ranked birds, which are the cause of the turn. In Fig. S7 we also show the distinction between outwards and inwards deviations from the common direction for two other events for which we noticed different pattern than the one discussed here. In particular, for event E12, the turn follows the joining of two separate flocks shortly before which could be the reason for it differing from the observed standard scenario.

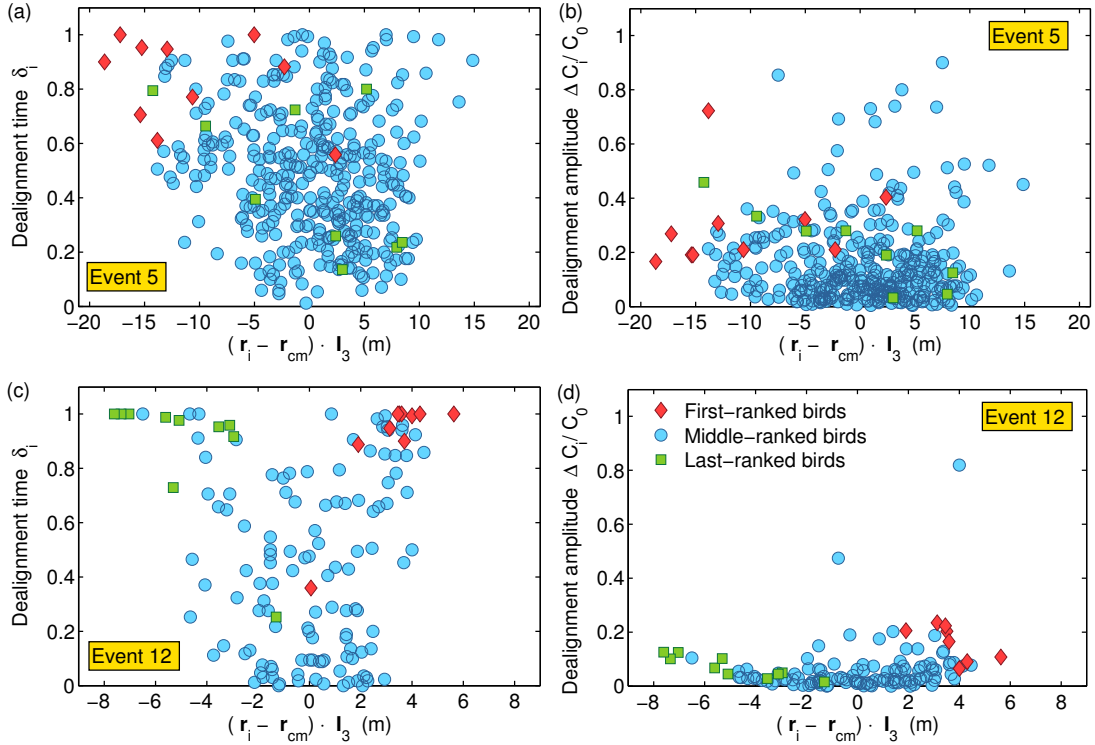


FIG. S6. **Deviations from the global direction of motion for different turning events.** We show deviations from average direction of motion for two turning events E5 and E12. (a), (c) Dealignment time factor $\delta_i(\tau)$ is plotted as a function of position of bird i along the longest elongation axis \mathbf{I}_3 , with respect to the flock's center of mass. On average, the farther away from the center of the flock a bird is, the longer time its directional correlation is lower than C_0 . The top ten ranked birds (red diamonds) are situated close to one edge, that is farthest away from the center of the flock along \mathbf{I}_3 axis, while last ten birds to turn (green squares) are close to the other edge of the flock or not, depending on a particular propagation of the turn through the flock. (b), (d) Dealignment amplitude $\Delta C_i/C_0$ is shown as a function of position of bird i along the longest elongation axis \mathbf{I}_3 , with respect to the flock's center of mass. No obvious dependence on the position is observed.

-
- [1] Attanasi A., Cavagna A., Del Castello L., Giardina I., Grigera T.S., Jelić A., Melillo S., Poh, O., Shen E., Viale M. Information transfer and behavioural inertia in starling flocks *Nat. Phys.* **10**, 691–696 (2014).
 - [2] M Ballerini, N Cabibbo, R Candelier, A Cavagna, E Cisbani, I Giardina, A Orlandi, G Parisi, A Procaccini, M Viale & V Zdravkovic, Empirical investigation of starling flocks: A benchmark study in collective animal behaviour. *Anim. Behav.* **76**, 201–215 (2008).
 - [3] A Cavagna, SM Duarte Queirós, I Giardina, F Stefanini & M Viale, Diffusion of individual birds in starling flocks. *Proc. R. Soc. B* **280**, 20122484 (2013).
 - [4] Lima, SL, Ecological and evolutionary perspectives on escape from predatory attack: a survey of North American birds *Wilson Bull.* **105**, 1–47 (1993).

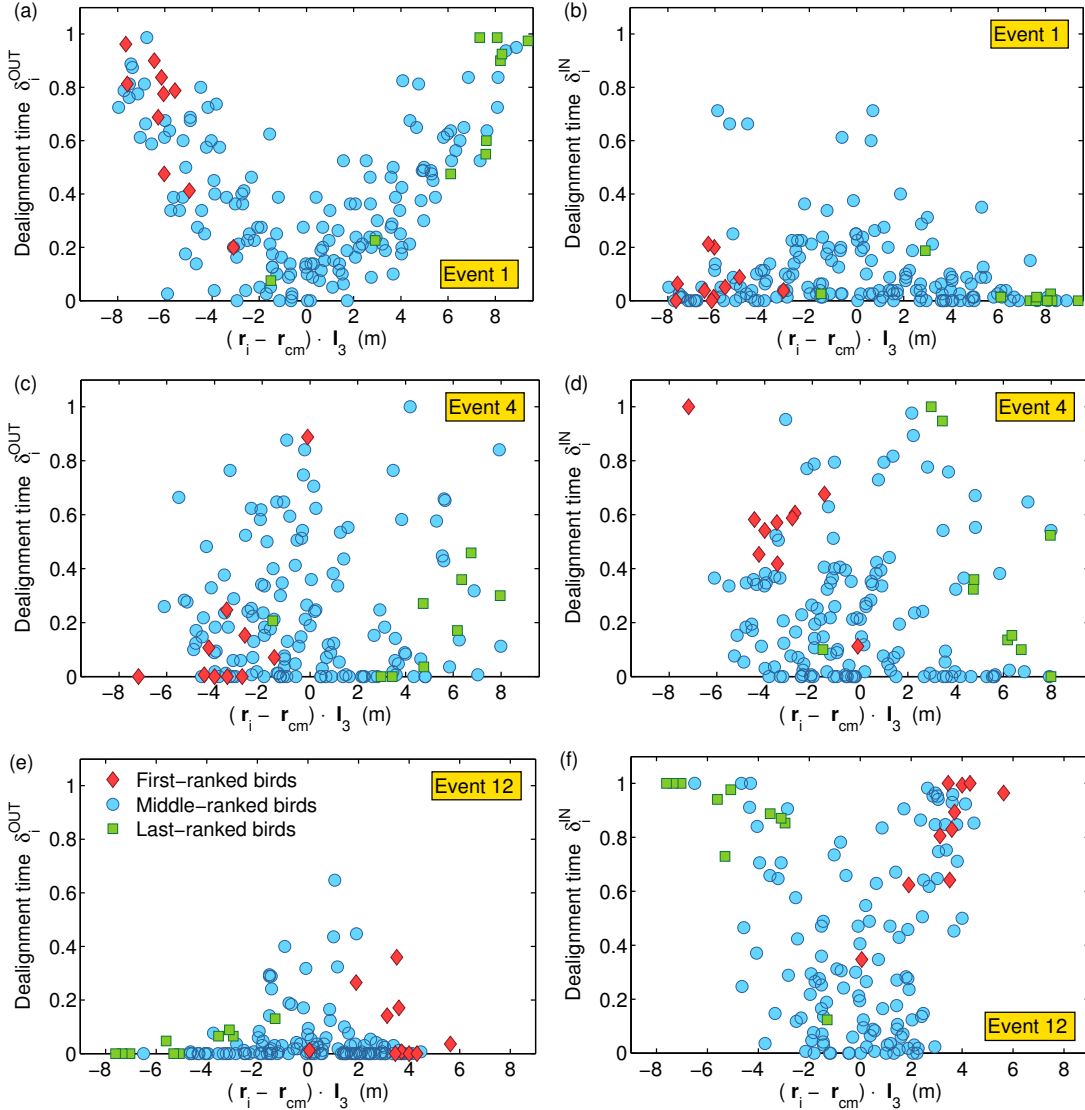


FIG. S7. **Outward and inward deviations with respect to the center of a flock.** For each bird i we separate deviations from the global direction of motion that are below the threshold value C_0 depending on whether they are directed outwards or inwards with respect to the center of the flock. Appropriate dealignment time factors δ_i^{out} and δ_i^{in} are shown in panels (a) and (b), respectively. The former one, δ_i^{out} , gives the percentage of time during time interval τ during which bird i was deviating stronger than C_0 and in the direction away (outwards) from the flock. The latter one, δ_i^{in} , presents the amount of time within τ that bird i was oriented more towards the center (inwards) of the flock. At each moment of time t , we separate outward and inward deviations using a plane defined by the direction of motion \mathbf{n}_1 and the longest elongation axis \mathbf{l}_3 . If within this plane we define a vector \mathbf{n}_\perp orthogonal to the direction of motion \mathbf{n}_1 , then the velocity deviations are calculated as $\mathbf{n}_\perp \cdot \mathbf{v}_i$. Depending on the position of the bird along the \mathbf{l}_3 axis with respect to the barycenter, and the deviation along \mathbf{n}_\perp , we can distinguish if a deviation is inwards or outwards. For event E1, the results show that most deviations by the birds on the sides are made in the direction away from the flock and are responsible for the increase in the flock's elongation in the transverse direction. This can be compared to the diffusion close to the wall, where in the case of a flock the birds on the side have more space to deviate towards the sides (away from the center), than towards the center of the flock where most of their neighbors are. The turn starts by deviations in the opposite direction—towards the inside of the flock—by the two top ranked birds shown in panel (b) with the highest δ_i^{in} among the top ranked birds (red diamonds). On the other hand, birds that are positioned in the center of the flock, do not show any preference for deviations towards inside or outside of the flock, since they themselves are at the central part of the flock. However, even though many of the events follow the trend as shown for event number E1, this is not always the case. For example, in event E4, there is no clear distinction between the outward and inward deviations. Finally, in event E12, we find a situation opposite to event E1, where most of the deviations are inwards, and the turn starts by repeated outward fluctuations.